# Prostaglandin D 2 Controls Local Blood Flow and Sleep-Promoting Neurons in the VLPO via Astrocyte-Derived Adenosine

Emeric Scharbarg, Augustin Walter, Laure Lecoin, Thierry Gallopin, Frédéric Lemaître, Manon Guille-Collignon, Nathalie Rouach, Armelle Rancillac

# Prostaglandin $D_2$ controls local blood flow and sleep-promoting neurons in the VLPO via astrocyte-derived adenosine

Emeric Scharbarg[1], Augustin Walter[2], Laure Lecoin[2], Thierry Gallopin[1], Frédéric Lemaître[3], Manon Guille-Collignon[3], Nathalie Rouach[2] & Armelle Rancillac[1,2]*

[1]Brain Plasticity Unit, CNRS, ESPCI-ParisTech, Labex Memolife, Université PSL, Paris, France. [2]Neuroglial Interactions in Cerebral Physiology and Pathologies, Center for Interdisciplinary Research in Biology, Collège de France, CNRS, Inserm, Labex Memolife, Université PSL, Paris, France. [3]PASTEUR, Département de Chimie, Ecole Normale Supérieure, PSL University PSL, Sorbonne Université, CNRS, 75005 Paris, France.

*To whom correspondence should be addressed: armelle.rancillac@college-de-france.fr

**One Sentence Summary:** Prostaglandin $D_2$ increases local blood flow and activates sleep-promoting neurons via astrocyte-derived adenosine in the VLPO.

**KEYWORDS:** Purine enzymatic biosensors, $PGD_2$ receptors ($DP_1R$), Neurovascular coupling, Sleep-promoting neurons, NREM sleep, Neuroglial Interactions, $A_{2A}$ receptors ($A_{2A}R$).

## ABSTRACT

Prostaglandin $D_2$ ($PGD_2$) is one of the most potent endogenous sleep-promoting molecules. However, the cellular and molecular mechanisms of the $PGD_2$-induced activation of sleep-promoting neurons in the ventrolateral preoptic nucleus (VLPO), the major non-rapid eye movement (NREM)-sleep center, still remains unclear. We here show that $PGD_2$ receptors ($DP_1$) are not only expressed in the leptomeninges, but also in astrocytes from the VLPO. We further demonstrate, by performing real-time measurements of extracellular adenosine using purine enzymatic biosensors in the VLPO, that $PGD_2$ application causes a 40% increase in adenosine level, via an astroglial release. Measurements of vasodilatory responses and electrophysiological recordings finally reveal that in response to $PGD_2$ application, adenosine release induces an $A_{2A}R$-mediated dilatation of blood vessels and activation of VLPO sleep-promoting neurons. Altogether, our results unravel the $PGD_2$ signaling pathway in the VLPO, controlling local blood flow and sleep-promoting neurons, via astrocyte-derived adenosine.


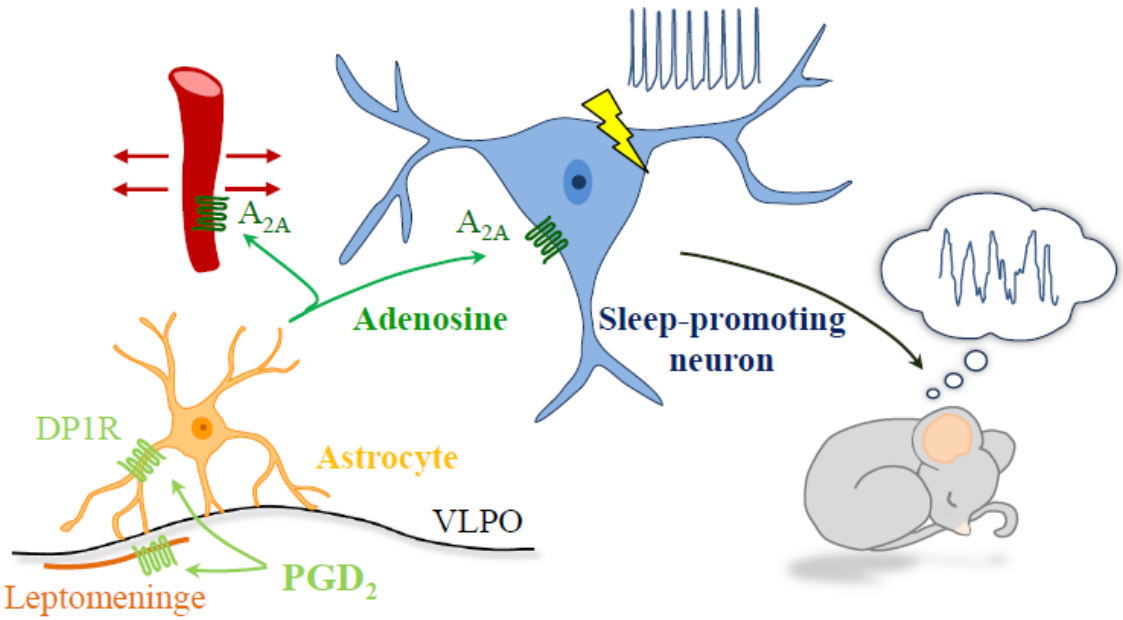

## INTRODUCTION

Prostaglandin $D_2$ ($PGD_2$) is the most potent endogenous sleep-promoting molecule[1–4]. Its concentration in cerebrospinal fluid exhibits a circadian variation synchronized with the sleep-wake cycle[5]. Immunofluorescence labeling and *in situ* hybridization have shown that $PGD_2$ receptors ($DP_1R$) are almost exclusively expressed in some arachnoid trabecular cells of the basal forebrain[6,7]. Activation of $DP_1R$ by $PGD_2$ infusion via microdialysis probe was further shown to induce adenosine release in a dose-dependent manner in the subarachnoid space of the basal forebrain and to promote sleep via adenosine $A_{2A}$ receptor ($A_{2A}R$) activation. Pretreatment with a specific adenosine $A_{2A}R$ antagonist indeed reduces the amount of $PGD_2$-induced sleep[7]. In vivo administration of $PGD_2$ by microdialysis probes was tested in various rat brain regions and identified the ventral surface of the rostral basal forebrain as the most effective area in promoting non-rapid eye movement (NREM) sleep[1,4], which was reduced by adenosine $A_{2A}$ antagonist[8]. However, combining $PGD_2$ infusion with c-Fos immunolabelling revealed c-Fos-immunoreactivity in the ventrolateral preoptic nucleus (VLPO), the major NREM sleep center[9], whereas the basal forebrain remained unlabeled[3].

Therefore, although several key aspects regarding $PGD_2$-induced sleep have been elucidated, our understanding of its physiological mechanisms is still incomplete. The VLPO being a very small brain structure, deeply localized, and not anatomically well-defined, complicate its investigation. This study thus here aims to decipher how locally in the VLPO, $PGD_2$ leads to the activation of sleep-promoting neurons.

## RESULTS AND DISCUSSION

NREM sleep induction by $PGD_2$ infusion being completely dependent on the activation of its $DP_1$ receptor[2], we first investigated the expression of this receptor in the VLPO (Fig. 1). Confirming previous reports from the literature, we also observed strong immunostaining on the leptomeninges at the border of the VLPO. However, we also find an immunolabelling into the VLPO (Fig. 1A). We used GFAP-GFP-expressing mice, to further reveal whether astrocytes could indeed express the $DP_1$ receptor. This transgenic mouse line has the interesting property to have only some astrocytes expressing GFP, not all of them, allowing better identification of individual cells. For the first time, we revealed that almost all GFP-GFAP-labeled VLPO astrocytes are expressing $DP_1R$, with a dense expression on the somata and primary processes (Fig. 1B,C).

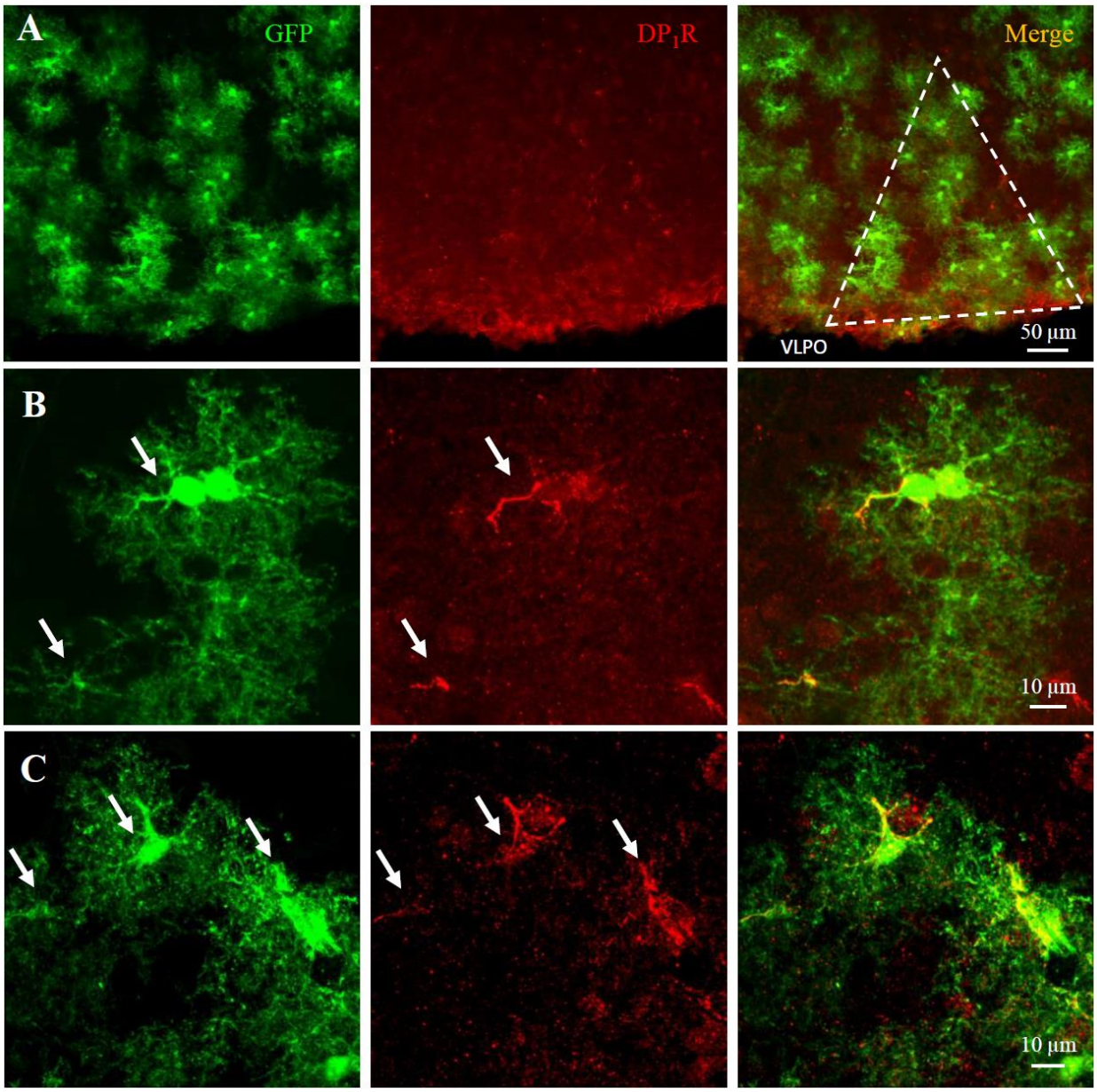


**Figure 1. Astrocytes in the VLPO express $DP_1R$. A,** Confocal images showing immunostaining of $DP_1R$ (in red) in the leptomeninges and the VLPO, as highlighted by a white dashed triangle. **B** and **C**, Confocal images reveal that astrocytes from GFAP-GFP mice (in green) are also expressing $DP_1R$ (in red). White arrows indicate regions of strong co-labeling.

Next, to assess whether an increased level of $PGD_2$ is also associated with adenosine released in the VLPO, we performed real-time measurements of extracellular adenosine using purine enzymatic biosensors on brain slices[10–13] (Fig. 2). Measurements with adenosine (ADO) probes

represent total purinergic responses and were referred to as ADO' (Fig. 2B). In the VLPO, we measured a basal ADO' level of 2.24 ± 0.22 µM, which significantly increased to 3.13 ± 0.35 µM under $PGD_2$. ADO's level decreased to 2.23 ± 0.44 µM after the wash (Fig. 2C,D). These experiments were then reproduced using INO biosensors to evaluate the proportion of inosine and its metabolites in the ADO' recording. We measured a variation from 1.13 ± 0.042 to 1.53 ± 0.13 µM in response to $PGD_2$, indicating that approximatively ~50% of the ADO' signal was specific to adenosine.

To further investigate whether adenosine is released by astrocytes in response to $PGD_2$, we performed real-time ADO measurements in pre-treated slices and continuously perfused with the glial toxin fluoroacetate (FAC; 5 mM). As shown in figure 2D, FAC treatment completely abolished the adenosinergic tone below the detection limit of the probe, as well as the ADO response to $PGD_2$ application (0.1 ± 0.1 µM; Fig. 2D). This result points to the role of glial cells as essential effectors of the $PGD_2$-dependent increase in extracellular ADO levels.

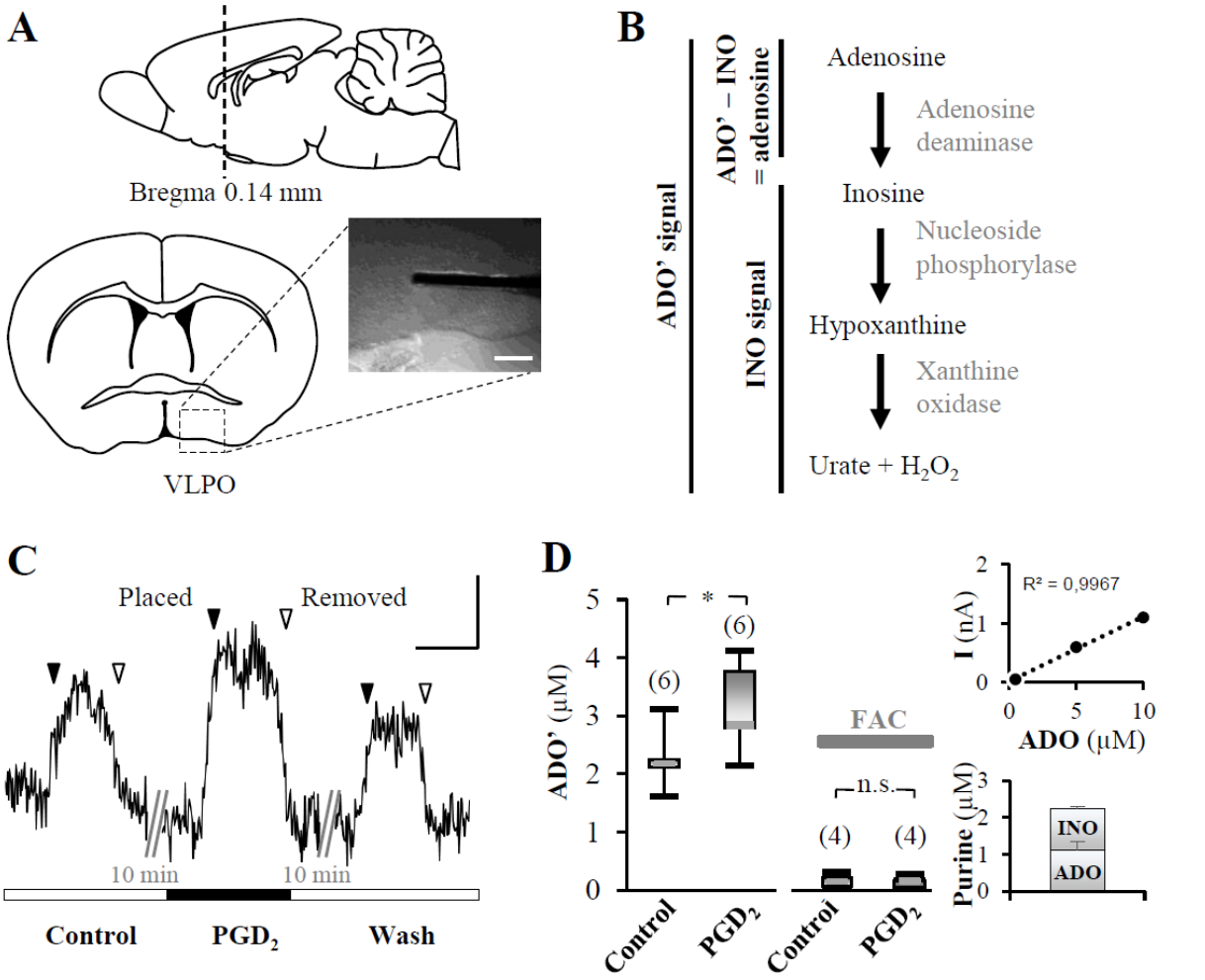


**Figure 2.** ***In situ*** **measurements of astrocytic-derived adenosine in response to $PGD_2$ application in the VLPO.** (**A**) Sagittal schematic representation of the mouse brain (top) and a VLPO slice at Bregma 0.14 mm (bottom). Photomicrograph of an ADO biosensor within the VLPO. Scale bar: 180 µm. (**B**) Enzymatic cascades used to measure adenosine and inosine. Adenosine biosensor measurements give a total purinergic concentration of adenosine and its metabolites called ADO'. The signal of INO is thereafter subtracted to obtain the ADO signal. (**C**) Representative recording of real-time ADO' signals within the VLPO. ADO biosensors were lowered into the VLPO area ('Placed'; black arrowheads) and raised ('Removed' white arrowheads) successively in control, 1 µM of $PGD_2$, and after 10 minutes wash back again into the tissue to prevent the probe desensitization. Scale bare: 1 min, 0.05 nA. (**D**) Left: box plots of the ADO' measurements in the control condition, under $PGD_2$ (1 µM) and in the presence of fluoroacetate (FAC; 5 mM), a glial toxin. The median is plotted as the central gray bar of the box, the upper and lower quartiles are the edges of the box and the whiskers show the extremes of the distribution. Sample sizes are indicated in parentheses. Right: example of a calibration curve from the adenosine biosensor showing a linear response from 1 to 10 µM adenosine (top), with ratios of ADO ($n$ = 6) and INO ($n$ = 3) detected in the VLPO in the control condition (bottom). *$P$ < 0.05, Wilcoxon matched-pairs signed rank test.

Adenosine is a potent vasodilator acting on vascular adenosine $A_{2A}$ receptors ($A_{2A}R$)[14,15]. We thus investigated the putative release of adenosine in response to $PGD_2$ application by recording blood vessel diameter changes in the VLPO (Fig. 3). We found that $PGD_2$ reversibly dilated intraparenchymal arterioles within the VLPO, by 12.17 ± 3.93% ($n$ = 7; $P \leq 0.001$; Wilcoxon test, Fig. 3). This response was blocked in the presence of a selective $A_{2A}R$ antagonist (ZM241385; 10 µM, $n$ = 5; $P$ = 0.125, Wilcoxon test, Fig. 3B,C), and was also significantly impaired compared to control condition ($P < 0.01$; Mann-Whitney $U$-test, Fig. 3C), indicating that $PGD_2$ induces adenosine-mediated signaling.

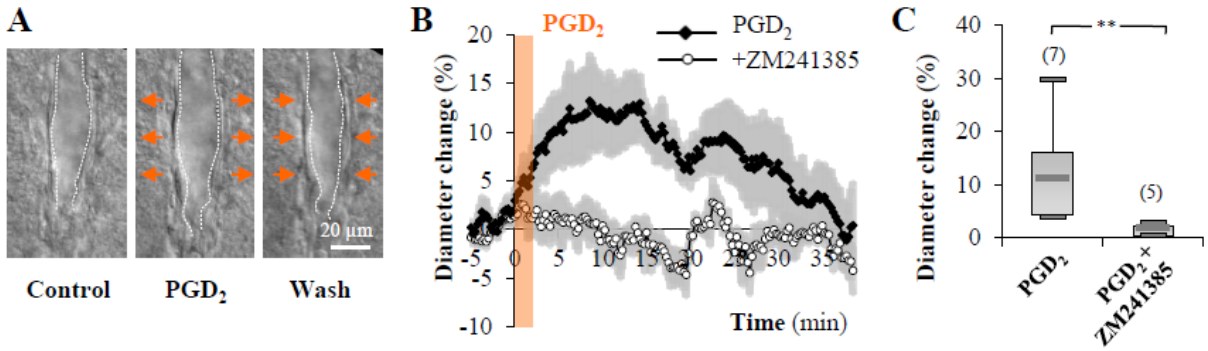


**Figure 3. $PGD_2$ induces $A_{2A}R$-mediated vasodilation in the VLPO.** (**A**) Photograph of a vascular response induced by bath application of $PGD_2$ (1 µM; 2 min). The dotted white lines highlight the inner diameter of the blood vessel. (**B**) Mean ± SEM vascular responses induced by 2 min application of $PGD_2$ alone (black diamond; $n$ = 7) or in the presence of ZM241385, an $A_{2A}$ receptor antagonist (open circle; $n$ = 5). (**C**) Box plots of the vascular response measured at 9-10 min after $PGD_2$ application onset. The median is plotted as the central grey bar of the box, the upper and lower quartiles are the edges of the box and the whiskers show the extremes of the distribution. Sample sizes are indicated in parentheses. $^{**}P < 0.01$; Mann-Whitney $U$-test.

Several reports have suggested that increased adenosine levels can modulate the activity of adenosine $A_{2A}R$–expressing neurons in the VLPO[2,11,16–18]. To further investigate whether $PGD_2$ can induce neuronal depolarization within the VLPO, we performed patch-clamp recordings of sleep-promoting neurons in response to the bath application of $PGD_2$ (Fig. 4A,B). To identify sleep-

promoting neurons in the VLPO, we used a transgenic mouse selectively expressing the green fluorescent protein (GFP) in galanin-expressing neurons (Gal-GFP mice). Galanin is indeed a reliable chemical marker of sleep-promoting neurons in the VLPO and allows clear identification of these neurons in an acute slice preparation[19–21].

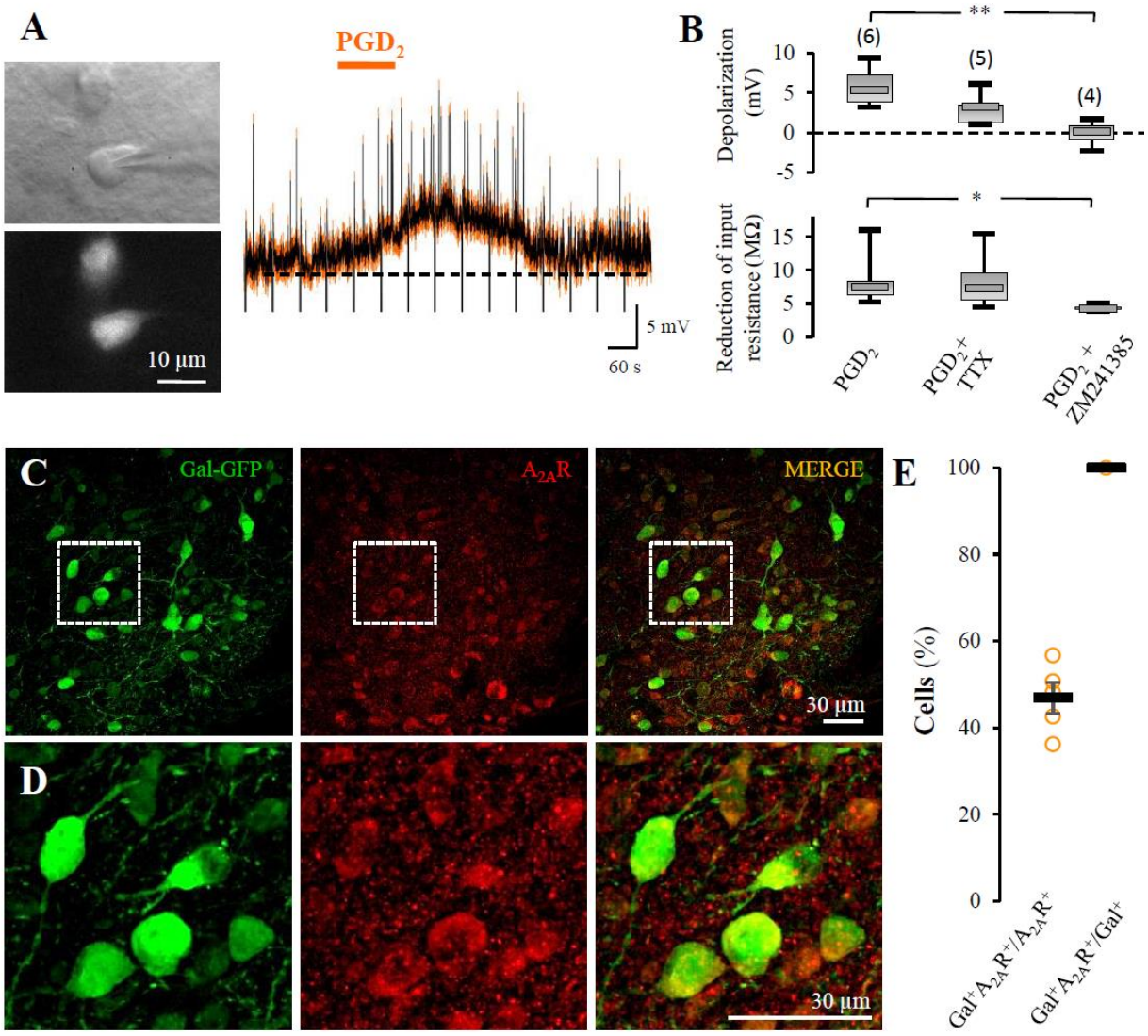


**Figure 4. $PGD_2$ depolarizes Gal-GFP neurons via $A_{2A}R$ activation.** (**A**) Left: epifluorescence and infrared images of the recorded Gal-GFP neuron. Right: mean (black) ± SEM (orange) electrophysiological response in current-clamp of a Gal-GFP neuron to $PGD_2$ application (1 µM; 2 min, n = 6). The black dashed bar indicated the membrane potential of -58 mV. (**B**) Box plots of the depolarizations induced by $PGD_2$ (top) and of the reduction of the input resistance (bottom).

The median is plotted as the central grey bar of the box, the upper and lower quartiles are the edges of the box and the whiskers show the extremes of the distribution. Sample sizes are indicated in parentheses. (**C**) Confocal images showing the expression of $A_{2A}R$ (red) in Gal-GFP neurons (green) and their merge (orange). (**D**) Confocal zooms of ROIs are indicated by dashed white squares in C. (**E**) Plots of means of labeled cells per animal (orange circles, $n = 5$) and the global mean (black bar). $^{**}P < 0.01$, ANOVA and Kruskal-Wallis mutli-comparisons test.

Patch-clamp recordings of Gal-GFP neurons showed that $PGD_2$ application induces a significant membrane depolarization of $5.79 \pm 0.98$ mV ($n = 6$; $P < 0.05$, Wilcoxon test; Fig. 4A,B). Additionally, their input resistance was reduced by 8.77% (from $977.68 \pm 66.89$ to $891.95 \pm 54.85$ MΩ) in response to $PGD_2$ application. The depolarizing effect of $PGD_2$ persisted in the presence of TTX and was not statistically reduced compared to the one induced in the absence of TTX ($3.04 \pm 0.92$ mV, $n = 5$; $P = 0.515$, ANOVA and Kruskal-Wallis multi-comparisons test; Fig. 4B). Moreover, PGD2 application in the presence of TTX still reduces neuronal input resistances by 8.86% (from $1183.19 \pm 168.05$ to $1078.39 \pm 148.51$ MΩ) indicating a direct effect of $PGD_2$ on sleep-promoting neurons. However, in the presence of an adenosine $A_{2A}R$ antagonist, ZM241385, the depolarization induced by $PGD_2$ was blocked ($-0.08 \pm 0.85$ mV; $n = 4$; $P < 0.01$, ANOVA and Kruskal-Wallis multi-comparisons test; Fig. 4B) and the reduction of the input resistance significantly less reduced, by 4.37% (from $9886.78 \pm 92.32$ to $943.67 \pm 88.50$ MΩ; ANOVA and Kruskal-Wallis multi-comparisons test; Fig. 4B). These data further show that in the VLPO, $PGD_2$ induces adenosine release which could then activate $A_{2A}R$ on sleep-promoting neurons.

The presence of $A_{2A}R$ on sleep-promoting neurons was previously suggested either pharmacologically by electrophysiological recordings[11,17], or molecularly using $A_{2A}$ receptor-deficient mice[22] or using sleep-wake behavior analyses associated with c-Fos-IR quantification in

the VLPO[18]. To firmly demonstrate that these receptors are indeed expressed by sleep-promoting neurons, we performed the immunostaining of $A_{2A}R$ and found that nearly all Gal-GFP neurons expressed this receptor, and ~ 50% of $A_{2A}R$ expressing cells were Gal-GFP ($n$ = 5, Fig. 4C,D). This result indicates that sleep-promoting neurons of the VLPO also express $A_{2A}R$. Taken together, the results of this study clearly define the cellular and molecular signaling pathway of $PGD_2$ in VLPO.

Here, we demonstrate and quantify for the first-time adenosine release in response to $PGD_2$ application into the VLPO. In addition, we established that astrocytes are crucial elements involved in increased levels of adenosine. These cells express $DP_1R$ to sense $PGD_2$ accumulation during wakefulness and their alteration using FAC abolishes adenosine release. Finally, we show that in response to $PGD_2$ application, adenosine release simultaneously induces $A_{2A}R$-mediated vasodilation and depolarization of sleep-promoting neurons. Altogether, our results provide new evidence regarding $PGD_2$ regulation of neuronal activity in the VLPO.

Using amperometric biosensors on mouse VLPO slices, we directly demonstrated that extracellular adenosine is increased in response to $PGD_2$ application. Previous microdialysis analysis already reported extracellular adenosine release in response to $PGD_2$ infusion, but only in the subarachnoid space of the basal forebrain[7]. Indeed, the small size of the VLPO does not facilitate its study. However, $PGD_2$ is a fat-soluble molecule. This paracrine signaling agent can diffuse into the brain tissue. The accumulation of $PGD_2$ during the day will then activate astrocytes via $DP_1Rs$ and induce adenosine release. It has indeed already been shown that $PGD_2$-induced increase in extracellular adenosine is absent in mice lacking the $DP_1R$, indicating that activation of these receptors is required for this increase of adenosine[7].

In this study, we found that approximately 50% of the ADO' signal was specific to adenosine, which is similar to previous studies. However, the basal adenosine levels we measured in this study seem higher than those recorded in the basal forebrain[13], which probably results from different experimental protocols. Quantification of extracellular adenosine levels in the presence of FAC, a molecule known to block cell metabolism, further revealed an astrocytic source of adenosine. As FAC is preferentially taken up by astrocytes relative to neurons[23], the abolition of adenosinergic tone in the VLPO by FAC suggests an astrocyte-derived adenosine release in response to $PGD_2$ application. However, we cannot exclude that the release of a paracrine mediator by the leptomeninges may also participate in astrocyte activation.

Here, we did not investigate how extracellular adenosine levels were increased. Many pathways can indeed regulate extracellular adenosine levels, including adenosine exocytosis[24], concentrative nucleoside transporters (CNTs), or transporters such as equilibrative nucleoside transporters (ENTs)[25]. Alternatively, ATP can also be released by astrocytes, via $P_2X_7$ receptors or hemichannels and converted into adenosine following a degradative enzymatic activity from ectonucleotidases. This latest mechanism was recently proposed in the VLPO following the photostimulation of astrocytic channelrhodopsin-2[26]. Future work would be required to elucidate the molecular pathways underlying extracellular adenosine release in the VLPO in response to $PGD_2$.

In the VLPO, adenosine then acts on both $A_1$ and $A_{2A}R$. In particular, $A_1R$ is widely expressed, by local GABAergic interneurons, whose activation is proposed to indirectly promote sleep via disinhibition of sleep-promoting neurons[17,26–28]. Regarding $A_{2A}R$, their expression on blood vessels is well established[15]. However, their expression by sleep-promoting neurons was only indirectly

suggested by c-Fos protein immunoreactivity, pharmacological blockade or activation, electrophysiological recordings, as well as by the use of KO mice[11,17,18,29,30]. Here, we demonstrate for the first time by immunolabelling that $A_{2A}R$ is indeed expressed by sleep-promoting neurons in the VLPO. Moreover, our study also highlights a key role for $PGD_2$ in the neurovascular coupling (NVC), linking via $A_{2A}R$ activation, vasodilation, and increased neuronal activity of sleep-promoting neurons. The tight link between blood flow regulation and neuronal activity is essential for normal brain function. This result strengthens the role of prostaglandins in the NVC. Prostaglandin E2 was indeed also reported to be in the cortex, a key vasoactive messenger of NVC responses to sensory stimulation[31].

$A_{2A}R$ immunolabelling here reveals that all sleep-promoting neurons express this receptor in mice. This result contrasts with previous reports in rats, where the depolarizing effect of $A_{2A}R$ was only observed in a subset of sleep-promoting neurons[17]. However, this is consistent with our previous study in mice, showing that adenosine as well as an $A_{2A}$ agonist were able to depolarize all recorded sleep-promoting neurons[11]. The expression of $A_{2A}R$ on sleep-promoting neurons was further confirmed in mice, by the depolarizing effect of $PGD_2$ on sleep-promoting neurons, which is prevented in the presence of the $A_{2A}R$ antagonist. However, we cannot exclude the possibility that sleep-promoting neurons could also express $A_1R$. Indeed, adenosine release is well known to decrease the inhibitory tonus exert by local $A_1R$-expressing interneurons on sleep-promoting neurons, thereby favoring their depolarization[27]. But simultaneously, direct activation of $A_1R$ on sleep-promoting neurons would counterbalance the indirect disinhibition by the interneurons. As in the presence of ZM241385, $PGD_2$ does not affect sleep-promoting neurons, this supposes that $A_1R$ is also expressed, as observed in rats[17]. Consequently, in the presence of TTX, which blocks

the disinhibition of sleep-promoting neurons by interneurons, sleep-promoting neurons are still directly inhibited by $A_1R$ activation, while they are depolarized by $A_{2A}R$. Thus, the global response to $PGD_2$ tends to decrease compared to the control condition.

In summary, we have here demonstrated that astrocytes express $DP_1R$ in the VLPO, and regulate adenosine levels in response to $PGD_2$ application. Then, adenosine increases the blood flow and depolarizes sleep-promoting neurons, via $A_{2A}R$. Activation of the VLPO would then lead to the inhibition of the wake-promoting structures, resulting in sleep.

## METHODS AND MATERIALS

**Animals.** Male-only C57BL/6 mice (Charles River, France) of P40-60 days old, were used to analyze the vascular effect of $PGD_2$ and perform ADO measurements. FVB Gal-GFP mice (Mutant Mouse Regional Resource Center (MMRRC), USA) of P40-60 days old, were used for patch-clamp recordings. FVB Gal-GFP[32] and GFAP-GFP[33] mice, P40-60 days old, male-only, were used for immunostainings.

The Gal-GFP mouse strain used for this research project, STOCK Tg(Gal-EGFP)HX109Gsat/Mmucd, identification number 016342-UCD, was obtained from the MMRRC, an NIH-funded strain repository, and was donated to the MMRRC by the NINDS funded GENSAT BAC transgenic project. All animals were housed in a temperature-controlled (20-22°C) room under a 12-hour light-dark cycle with lights on at 08:00 a.m. All animals had *ad libitum* access to food and water. All animal procedures were conducted in strict compliance with our institutional protocols and were approved by the European Community Council Directive of 22 September 2010 (010/63/UE) and the local ethics committee (Comité d'éthique en matière d'expérimentation animale number 59, C2EA-59, 'Paris Centre et Sud'). Accordingly, the number of animals in our study was kept to the necessary minimum.

**Immunohistochemistry and Confocal Microscopy.** Mice were deeply anesthetized with Euthasol Vet (Pentobarbital, DECHRA) and perfused intracardially with paraformaldehyde (PFA 2%), between Zeitgeber Time (ZT) -1 and 3, so between 1 and 3 hours after the light was switched on in the animal house. The brains were carefully dissected and post-fixed overnight with PFA 2% at 4 °C. The next day, PFA was removed and the brains were cryoprotected overnight in PBS containing 30% sucrose. The brains were then cut into 40 µm sections with a

freezing microtome (HM 450, Thermo Fisher Scientific). Slices were stored in PBS at 4 °C until use. For immunohistochemistry, slices were washed 3 times 15 min in PBS 1X at room temperature (RT) and antigen retrieval was performed by incubating slices in 50 mM sodium citrate (147 mg trisodiumcitrate di-hydrate in 10 mL water, pH 8.5-9.0) preheated at 80 °C for 30 min. Slices were washed 3 times 15 min at RT with PBS 1X and incubated 24 h at RT with primary antibodies ($A_{2A}R$: AAR-002, polyclonal rabbit, Alamone Labs at 1:500; GFP: Abcam, Chicken, ab13970 at 1:500; $DP_1R$: ADI-905-800-100, polyclonal rabbit, Enzo at 1:500; GFP: AVES lab, Chicken at 1:1000 in PBS 1X / Triton X100 0.5% / 0.02% $NaN_3$) and then 4 nights at 4°C. Anti-adenosine $A_{2A}$ receptor is a highly specific antibody directed against the (C)RQLKQMESQPLPGER epitope of the mouse protein, corresponding to amino acid residues 201-2015 of the 3rd intracellular loop of mouse adenosine $A_{2A}$ receptor. $PGD_2$ receptor (DP1) polyclonal antibody the immunogen sequence used was NESYRCQTSTWV, corresponding to the N-terminus of $DP_1$, amino acids 2-23[34].

Slices were rinsed 3 times 15 min in PBS 1X at RT and incubated with secondary antibodies ($A_{2A}R$: A21429, goat-Alexa Fluor 555, Life Technologies at 1:1000; GFP: A11032, goat-Alexa Fluor 488, Invitrogen, 1:1000; DP1: goat anti-chicken 488 at 1:500; goat anti-rabbit 647 at 1:500 in PBS 1X / Triton X100 0.5% / 0.02 % $NaN_3$) for 48 h at 4°C. Slices were then washed 3 times 15 min with PBS 1X at RT, incubated with DAPI (1:1000) 20 min at RT, and washed again 10 min at RT before mounting with Fluoromount-G (00-4958-02, Invitrogen). For each immunostaining, a minimum of 4 fields per animal were acquired at the 25X and 63X objective (spinning disk W1, Zeiss Axioobserver Z1 with motorized XYZ stage; CSUW11 (Yokogawa) spinning-disk scan head). $GFP^+$, $A_{2A}^+$ and $DP1^+$ cells were counted manually in at least 1 region of interest (ROI) per slice per animal and at least in 3 mice. Then, a Z-stack of 30 µm thick with a 2 µm step was made

on each field. Acquisitions parameters were strictly conserved throughout different animals. Fluorescence cells were then counted on a maximal-intensity Z-projection image. The presented data corresponds to the average of all ROIs fluorescence intensities per condition. Image analyses were made using Fiji and ImageJ softwares (National Institute of Health, United States).

**Hypothalamic Slices.** Mice were rapidly decapitated between Zeitgeber Time (ZT)-1 and 3 and brains were quickly removed and placed into cold (~ 4°C) artificial cerebrospinal fluid (aCSF) containing (in mM): 130 NaCl; 5 KCl; 2.4 $CaCl_2$; 20 $NaHCO_3$; 1.25 $KH_2PO_4$; 1.3 $MgSO_4$; 5 D-glucose; and 15 sucrose (pH = 7.35). Brains were constantly oxygenated with 95% $O_2$ – 5% $CO_2$. During slicing, 1 mM kynurenate was added to the aCSF. Coronal brain slices (300 µm thick) containing the VLPO were cut with a vibratome (VT1200°S; Leica) and transferred to a constantly oxygenated (95% $O_2$ – 5% $CO_2$) holding chamber containing aCSF. Next, individual slices were placed in a submerged recording chamber maintained at 32°C and perfused (1.5 ml/min) with oxygenated kynurenate-free aCSF. Blood vessels were visualized using infrared videomicroscopy, with Dodt gradient contrast optics (Luigs and Neumann) mounted on an upright microscope (Zeiss) equipped with a CDD camera (Hamamatsu).

**Purine Biosensor Recording.** Purine biosensors (Sarissa Biomedical, Coventry, United Kingdom) were used to detect extracellular levels of either adenosine (ADO) or inosine (INO). Each biosensor included a platinum wire 50 µm in diameter and 0.5 mm in length, coated with a permselective layer and an enzymatic matrix surrounding the platinum electrode[10,35]. For the ADO biosensors, the enzymatic layer contained nucleoside phosphorylase, xanthine oxidase, and adenosine deaminase, whereas the INO biosensors lacked adenosine deaminase and were sensitive

to adenosine. Amperometric measurements started when hydrogen peroxide oxidized the platinum wire to create an electrical signal proportional to the purine concentration. Measurements with adenosine biosensors gave a total purinergic concentration of adenosine and its metabolites referred to as ADO[35,36]. In contrast, INO sensors were used to measure the response to inosine and its metabolites in a separate set of experiments, due to the small size of the VLPO. We thus obtained a specific ADO signal by subtracting the signal of INO sensors from ADO sensors; approximately 51% of the signal from the ADO/INO biosensor was specific to adenosine in our conditions. Before use, all biosensors were rehydrated in a buffer containing (in mM): 100 NaCl, 50 Tris, 20 glycerol, 1 $MgCl_2$, and 1 $CaCl_2$. All biosensor sets were calibrated at the beginning and end of each experiment with 10 µM adenosine or inosine. The ADO and INO recordings were performed after a 30 min stabilization period. The sensors were inserted sequentially during a 3 min period in the VLPO in aCSF: without $PGD_2$ (control condition), followed by $PGD_2$ (1 µM), and again after 10 min wash without $PGD_2$. The biosensors were placed in contact with the surface of the slice by micromanipulators, which was visually confirmed as a slight deformation on its surface, indicating that the electrode was properly embedded. During the experiment, microelectrode biosensors were polarized at +500 mV versus Ag/AgCl. Purine concentrations were assessed by subtracting the electrical signal of the sensor when inserted into the VLPO from the mean of the electrical signals measured 30 s before and after the insertion. The biosensor signals were acquired with an amperometric detector (AMU 110; Radiometer Analytical, Villeurbanne, France) using an acquisition board (Digidata 1322A; Molecular Devices) attached to a computer running the pCLAMP 9.2 software package (Molecular Devices). Analyses were performed using Clampfit (Molecular Devices), SigmaPlot (Systat), and Python software programs.

**Vascular Reactivity.** Blood vessels in the VLPO within the focal plane that exhibited a well-defined luminal diameter (10-20 µm) were selected for vascular reactivity. Images of blood vessels were acquired every 15 s with the Media Cybernetics software. The eventual drift of the images during the recording time was corrected either online for the z-drift or offline for the x and y axes using Image Pro Plus 7.0. Manual replacement of images to minimize the differences between two consecutive frames was performed using a subtraction tool from Image Pro Plus. To determine the location with the most movement, luminal diameters were quantified at different locations along the blood vessel using custom-written routines running within IgorPro (Wavemetrics). Control baselines were determined for 5 min at the start of the recording, with temperature maintained at 32 ± 1°C. Unresponsive blood vessels or vessels with unstable baselines were discarded from the analysis. Vessels were considered unstable when their diameter moved more than 5% during the control baseline test. Only one vessel per slice was recorded.

Vasomotor responses were expressed as percentages of the mean baseline diameter, 5 min before the switch with the solution containing $PGD_2$. Pharmacological effects were then analyzed by performing statistical comparisons between the 1 min period before $PGD_2$ application and the mean blood vessel diameter change at 9-10 min after $PGD_2$ application onset.

**Electrophysiological Recordings.** Electrophysiological experiments were performed at 32 ± 1°C using a MultiClamp700B (Axon Instruments) amplifier connected to an acquisition board (Digidata 1440; Axon Instruments), filtered at 5 kHz, digitized at 50 kHz, and recorded to a computer running pCLAMP9.2 software (Axon Instruments). Data were analyzed offline using the Clampfit software (Molecular Devices).

*Patch-clamp recordings in whole-cell configuration.*

Current clamp recordings were made at resting membrane potential and without series resistance compensation. Patch-clamp pipettes (3–6 MΩ) were pulled from a borosilicate glass tube (1.5 mm o.d., 0.86 mm i.d.; Harvard Apparatus, France) on a horizontal puller (Model P-100; Sutter Instrument, Novato, USA), and were filled with the following (in mM): 144 K-gluconate; 1 $MgCl_2$; 0.5 EGTA; 10 HEPES at pH 7.2; 285–295 mOsm. A short hyperpolarizing current step was applied at the beginning of each sweep, every 60 s, to monitor changes in input resistance throughout the recordings. This protocol frequently triggered low-threshold spikes (LTS). The liquid junction potential of the patch pipette and the perfused extracellular solution was 11 mV and was not accounted for in the data. The pipette was slowly brought to the selected neuron to be recorded in whole-cell configuration using infrared videomicroscopy guidance. Data were rejected if the access resistance changed by more than 25% during the recording of the control period and data reduction was performed to reduce data handling. Membrane potentials were measured between 4 and 6 min after the onset of the drug application and over a 2-min period for baseline before $PGD_2$ application. Input resistances were measured by the application of short steps of hyperpolarization each minute.

**Drugs.** The selective $A_{2A}$ receptor antagonist ZM 241385 (4-(-2-[7-amino-2-{2-furyl}{1,2,4}triazolo{2,3-a} {1,3,5}triazin-5-yl-amino]ethyl)phenol; 100 µM; Merck) was used to investigate the molecular pathway of the $PGD_2$-induce neuronal depolarization. To block neuronal transmission, $PGD_2$ was applied in the presence of tetrodotoxin (TTX; 1 µM; Latoxan) as well as 10 min after TTX application onset. Glial metabolism was inhibited using fluoroacetate (FAC; 5 mM and 50 min of preincubation; Sigma). $PGD_2$, (5Z,9α,13E,15S)-9,15-Dihydroxy-11-oxoprosta-5,13-dien-1-oic-acid (1 µM, Sigma).

**Statistical Analyses.** Data are expressed as mean ± standard error of the mean (SEM) and represented as a box plot, where the median is plotted as the central bar of the box, the upper and lower quartiles are the edges of the box, and the whiskers show the extremes of the distribution. The statistical significance of the data was assessed using either parametric tests (paired *t*-test and Student's *t*-test) or non-parametric tests (Wilcoxon test and Mann-Whitney *U*-test), depending on whether the values from the considered data set followed a normal distribution or not.

## AUTHOR INFORMATION


### Corresponding Authors

Armelle Rancillac − *Brain Plasticity Unit, CNRS, ESPCI-ParisTech, Labex Memolife, Université PSL, Paris, France and Neuroglial Interactions in Cerebral Physiology and Pathologies, Center for Interdisciplinary Research in Biology, Collège de France, CNRS, Inserm, Labex Memolife, Université PSL, Paris, France.* Email: armelle.rancillac@college-de-france.fr orcid.org/0000-0003-1085-5929.

### Authors

Emeric Scharbarg – *Brain Plasticity Unit, CNRS, ESPCI-ParisTech, Labex Memolife, Université PSL, 75005 Paris, France.* orcid.org/0000-0002-1818-3971

Augustin Walter – *Neuroglial Interactions in Cerebral Physiology and Pathologies, Center for Interdisciplinary Research in Biology, Collège de France, CNRS, Inserm, Labex Memolife, Université PSL, 75005 Paris, France.* orcid.org/0000-0002-7426-2674

Laure Lecoin – *Neuroglial Interactions in Cerebral Physiology and Pathologies, Center for Interdisciplinary Research in Biology, Collège de France, CNRS, Inserm, Labex Memolife, Université PSL, 75005 Paris, France.* orcid.org/0000-0001-5259-4339

Thierry Gallopin – *Brain Plasticity Unit, CNRS, ESPCI-ParisTech, Labex Memolife, Université PSL, 75005 Paris, France.* orcid.org/0000-0002-9741-3738

Frédéric Lemaître – *PASTEUR, Département de Chimie, Ecole Normale Supérieure, PSL University PSL, Sorbonne Université, CNRS, 75005 Paris, France.* orcid.org/0000-0003-4424-0981

Manon Guille-Collignon – *PASTEUR, Département de Chimie, Ecole Normale Supérieure, PSL University PSL, Sorbonne Université, CNRS, 75005 Paris, France.* orcid.org/0000-0003-2510-5549

Nathalie Rouach – *Neuroglial Interactions in Cerebral Physiology and Pathologies, Center for Interdisciplinary Research in Biology, Collège de France, CNRS, Inserm, Labex Memolife, Université PSL, 75005 Paris, France.* orcid.org/0000-0002-5574-888

**Author Contributions**

E.S. performed the amperometric recordings, F.L. and M.G.-C. provided the equipment and expertise for the amperometric recordings, A.R. performed vascular reactivity and electrophysiological recordings, L.L. and A.W. performed the immunostainings. A.R. performed all the figures. A.R. supervised and coordinated research activities. A.R. wrote the manuscript. All authors reviewed, provided constructive comments and approved the final version of the manuscript. N.R. and T.G. acquired funding. All authors have agreed on the final version of the manuscript.

**Note**

The authors declare no competing financial interest.

**Acknowledgments.** This work was supported by the Centre National de la Recherche Scientifique (CNRS), the French Institute of Health and Medical Research (Inserm), ESPCI ParisTech, Bettencourt Schueller Foundation and the Collège de France. We thank all members of the animal house facility from the Collège de France.

## REFERENCES


(1) Ueno, R.; Ishikawa, Y.; Nakayama, T.; Hayaishi, O. Prostaglandin D2 Induces Sleep When Microinjected into the Preoptic Area of Conscious Rats. *Biochem Biophys Res Commun* **1982**, *109* (2), 576–582. https://doi.org/10.1016/0006-291X(82)91760-0.

(2) Urade, Y.; Hayaishi, O. Prostaglandin D2 and Sleep/Wake Regulation. *Sleep Med. Rev.* **2011**, *15* (6), 411–418.

(3) Scammell, T.; Gerashchenko, D.; Urade, Y.; Onoe, H.; Saper, C.; Hayaishi, O. Activation of Ventrolateral Preoptic Neurons by the Somnogen Prostaglandin D2. *Proc Natl Acad Sci U S A* **1998**, *95* (13), 7754–7759.

(4) Matsumura, H.; Nakajima, T.; Osaka, T.; Satoh, S.; Kawase, K.; Kubo, E.; Kantha, S. S.; Kasahara, K.; Hayaishi, O. Prostaglandin D2-Sensitive, Sleep-Promoting Zone Defined in the Ventral Surface of the Rostral Basal Forebrain. *Proc. Natl. Acad. Sci. U.S.A* **1994**, *91* (25), 11998–12002.

(5) Pandey, H. P.; Ram, A.; Matsumura, H.; Hayaishi, O. Concentration of Prostaglandin D2 in Cerebrospinal Fluid Exhibits a Circadian Alteration in Conscious Rats. *Biochem Mol Biol Int* **1995**, *37* (3), 431–437.

(6) Oida, H.; Hirata, M.; Sugimoto, Y.; Ushikubi, F.; Ohishi, H.; Mizuno, N.; Ichikawa, A.; Narumiya, S. Expression of Messenger RNA for the Prostaglandin D Receptor in the Leptomeninges of the Mouse Brain. *FEBS Lett* **1997**, *417* (1), 53–56. https://doi.org/10.1016/S0014-5793(97)01253-2.

(7) Mizoguchi, A.; Eguchi, N.; Kimura, K.; Kiyohara, Y.; Qu, W. M.; Huang, Z. L.; Mochizuki, T.; Lazarus, M.; Kobayashi, T.; Kaneko, T.; Narumiya, S.; Urade, Y.; Hayaishi, O. Dominant Localization of Prostaglandin D Receptors on Arachnoid Trabecular Cells in Mouse Basal Forebrain and Their Involvement in the Regulation of Non-Rapid Eye Movement Sleep. *Proc. Natl. Acad. Sci. U.S.A* **2001**, *98* (20), 11674–11679.

(8) Satoh, S.; Matsumura, H.; Suzuki, F.; Hayaishi, O. Promotion of Sleep Mediated by the A2a-Adenosine Receptor and Possible Involvement of This Receptor in the Sleep Induced by Prostaglandin D2 in Rats. *Proc. Natl. Acad. Sci. U.S.A* **1996**, *93* (12), 5980–5984.

(9) Von Economo, C. Sleep As a Problem of Localization. *J. Nerv. Ment. Dis.* **1930**, *71* (3), 249–259. https://doi.org/10.1097/00005053-193003000-00001.

(10) Llaudet, E.; Botting, N. P.; Crayston, J. A.; Dale, N. A Three-Enzyme Microelectrode Sensor for Detecting Purine Release from Central Nervous System. *Biosens. Bioelectron.* **2003**, *18* (1), 43–52.

(11) Scharbarg, E.; Daenens, M.; Lemaître, F.; Geoffroy, H.; Guille-Collignon, M.; Gallopin, T.; Rancillac, A. Astrocyte-Derived Adenosine Is Central to the Hypnogenic Effect of Glucose. *Sci Rep* **2016**, *6*, 19107. https://doi.org/10.1038/srep19107.

(12) Sims, R. E.; Dale, N. Activity-Dependent Adenosine Release May Be Linked to Activation of Na +-K+ ATPase: An in Vitro Rat Study. *PLoS One* **2014**, *9* (1). https://doi.org/10.1371/journal.pone.0087481.

(13) Sims, R. E.; Wu, H. H. T.; Dale, N. Sleep-Wake Sensitive Mechanisms of Adenosine Release in the Basal Forebrain of Rodents: An in Vitro Study. *PLoS One* **2013**, *8* (1), e53814. https://doi.org/10.1371/journal.pone.0053814.

(14) Ngai, A. C.; Coyne, E. F.; Meno, J. R.; West, G. A.; Winn, H. R. Receptor Subtypes Mediating Adenosine-Induced Dilation of Cerebral Arterioles. *Am J Physiol Heart Circ Physiol* **2001**, *280* (5), H2329-35.

(15) Ralevic, V.; Dunn, W. R. Purinergic Transmission in Blood Vessels. *Auton Neurosci* **2015**, *191*, 48–66. https://doi.org/10.1016/j.autneu.2015.04.007.

(16) Huang, Z.-L.; Urade, Y.; Hayaishi, O. Prostaglandins and Adenosine in the Regulation of Sleep and Wakefulness. *Curr Opin Pharmacol* **2007**, *7* (1), 33–38. https://doi.org/10.1016/j.coph.2006.09.004.

(17) Gallopin, T.; Luppi, P. H.; Cauli, B.; Urade, Y.; Rossier, J.; Hayaishi, O.; Lambolez, B.; Fort, P. The Endogenous Somnogen Adenosine Excites a Subset of Sleep-Promoting Neurons via A2A Receptors in the Ventrolateral Preoptic Nucleus. *Neuroscience* **2005**, *134*, 1377–1390.

(18) Kumar, S.; Rai, S.; Hsieh, K. Adenosine A2A Receptors Regulate the Activity of Sleep Regulatory GABAergic Neurons in the Preoptic Hypothalamus. *Am J Physiol* **2013**, *305* (1), R31-41.

(19) Gaus, S. E.; Strecker, R. E.; Tate, B. A.; Parker, R. A.; Saper, C. B. Ventrolateral Preoptic Nucleus Contains Sleep-Active, Galaninergic Neurons in Multiple Mammalian Species. *Neuroscience* **2002**, *115* (1), 285–294.

(20) Chauveau, F.; Claverie, D.; Lardant, E.; Varin, C.; Hardy, E.; Walter, A.; Canini, F.; Rouach, N.; Rancillac, A. Neuropeptide S Promotes Wakefulness through the Inhibition of Sleep-Promoting Ventrolateral Preoptic Nucleus Neurons. *Sleep* **2020**, *43* (1). https://doi.org/10.1093/sleep/zsz189.

(21) Kroeger, D.; Absi, G.; Gagliardi, C.; Bandaru, S. S.; Madara, J. C.; Ferrari, L. L.; Arrigoni, E.; Münzberg, H.; Scammell, T. E.; Saper, C. B.; Vetrivelan, R. Galanin Neurons in the Ventrolateral Preoptic Area Promote Sleep and Heat Loss in Mice. *Nat Commun* **2018**, *9* (1). https://doi.org/10.1038/s41467-018-06590-7.

(22) Urade, Y.; Eguchi, N.; Qu, W.-M.; Sakata, M.; Huang, Z.-L.; Chen, J.-F.; Schwarzschild, M. A.; Fink, J. S.; Hayaishi, O. Sleep Regulation in Adenosine A2A Receptor-Deficient Mice. *Neurology* **2003**, *61* (11 Suppl 6), S94–S96. https://doi.org/10.1212/01.WNL.0000095222.41066.5E.

(23) Keyser, D. O.; Pellmar, T. C. Synaptic Transmission in the Hippocampus: Critical Role for Glial Cells. *Glia* **1994**, *10* (4), 237–243. https://doi.org/10.1002/glia.440100402.

(24) Pascual, O.; Casper, K. B.; Kubera, C.; Zhang, J.; Revilla-Sanchez, R.; Sul, J.-Y.; Takano, H.; Moss, S. J.; McCarthy, K.; Haydon, P. G. Astrocytic Purinergic Signaling Coordinates Synaptic Networks. *Science* **2005**, *310* (5745), 113–116. https://doi.org/10.1126/science.1116916.

(25) Paes-De-Carvalho, R. Adenosine as a Signaling Molecule in the Retina: Biochemical and Developmental Aspects. *An Acad Bras Cienc* **2002**, *74* (3), 437–451. https://doi.org/10.1590/S0001-37652002000300007.

(26) Choi, I. S.; Kim, J. H.; Jeong, J. Y.; Lee, M. G.; Suk, K.; Jang, I. S. Astrocyte-Derived Adenosine Excites Sleep-Promoting Neurons in the Ventrolateral Preoptic Nucleus: Astrocyte-Neuron Interactions in the Regulation of Sleep. *Glia* **2022**, No. February, 1–22. https://doi.org/10.1002/glia.24225.

(27) Morairty, S.; Rainnie, D.; McCarley, R.; Greene, R. Disinhibition of Ventrolateral Preoptic Area Sleep-Active Neurons by Adenosine: A New Mechanism for Sleep Promotion. *Neuroscience*. 2004, pp 451–457.

(28) Chamberlin, N. L.; Arrigoni, E.; Chou, T. C.; Scammell, T. E.; Greene, R. W.; Saper, C. B. Effects of Adenosine on GABAergic Synaptic Inputs to Identified Ventrolateral Preoptic Neurons. *Neuroscience* **2003**, *119*, 913–918.

(29) Scammell, T. E.; Gerashchenko, D. Y.; Mochizuki, T.; McCarthy, M. T.; Estabrooke, I. V; Sears, C. a; Saper, C. B.; Urade, Y.; Hayaishi, O. An Adenosine A2a Agonist Increases Sleep and Induces Fos in Ventrolateral Preoptic Neurons. *Neuroscience* **2001**, *107* (4), 653–663.

(30) Huang, Z.-L.; Qu, W.-M.; Eguchi, N.; Chen, J.-F.; Schwarzschild, M. A.; Fredholm, B. B.; Urade, Y.; Hayaishi, O. Adenosine A2A, but Not A1, Receptors Mediate the Arousal Effect of Caffeine. *Nat Neurosci* **2005**, *8* (7), 858–859. https://doi.org/10.1038/nn1491.

(31) Lacroix, A.; Toussay, X.; Anenberg, E.; Lecrux, C.; Ferreiros, N.; Karagiannis, A.; Plaisier, F.; Chausson, P.; Jarlier, F.; Burgess, S. A.; Hillman, E. M. C.; Tegeder, I.; Murphy, T. H.; Hamel, E.; Cauli, B. COX-2-Derived Prostaglandin E2 Produced by Pyramidal Neurons Contributes to Neurovascular Coupling in the Rodent Cerebral Cortex. *Journal of Neuroscience* **2015**, *35* (34), 11791–11810. https://doi.org/10.1523/JNEUROSCI.0651-15.2015.

(32) Gong, S.; Zheng, C.; Doughty, M. L.; Losos, K.; Didkovsky, N.; Schambra, U. B.; Nowak, N. J.; Joyner, A.; Leblanc, G.; Hatten, M. E.; Heintz, N. A Gene Expression Atlas of the Central Nervous System Based on Bacterial Artificial Chromosomes. *Nature* **2003**, *425* (6961), 917–925. https://doi.org/10.1038/nature02033.

(33) Nolte, C.; Matyash, M.; Pivneva, T.; Schipke, C. G.; Ohlemeyer, C.; Hanisch, U.-K.; Kirchhoff, F.; Kettenmann, H. GFAP Promoter-Controlled EGFP-Expressing Transgenic Mice: A Tool to Visualize Astrocytes and Astrogliosis in Living Brain Tissue. *Glia* **2001**, *33* (1), 72–86. https://doi.org/10.1002/1098-1136(20010101)33:1<72::AID-GLIA1007>3.0.CO;2-A.

(34) Frenguelli, B. G.; Llaudet, E.; Dale, N. High-Resolution Real-Time Recording with Microelectrode Biosensors Reveals Novel Aspects of Adenosine Release during

Hypoxia in Rat Hippocampal Slices. *J Neurochem* **2003**, *86* (6), 1506–1515. https://doi.org/10.1046/j.1471-4159.2003.01957.x.

(35) Dale, N.; Pearson, T.; Frenguelli, B. G. Direct Measurement of Adenosine Release during Hypoxia in the CA1 Region of the Rat Hippocampal Slice. *J Physiol* **2000**, *526 Pt 1*, 143–155.